Progress in Oceanography 83 (2009) 208–216

Contents lists available at ScienceDirect

Progress in Oceanography

journal homepage: www.elsevier.com/locate/pocean

Lagrangian studies of phytoplankton growth and grazing relationships in a coastal upwelling ecosystem off Southern California

Michael R. Landry *, Mark D. Ohman, Ralf Goericke, Michael R. Stukel, Kate Tsyrklevich

Integrative Oceanography Division, Scripps Institution of Oceanography, University of California at San Diego, La Jolla, CA 92093, USA

ARTICLE INFO

Article history:
Received 17 July 2008
Received in revised form 22 January 2009
Accepted 16 July 2009
Available online 26 July 2009

ABSTRACT

Experimental studies of phytoplankton growth and grazing processes were conducted in the coastal upwelling system off Point Conception, California to test the hypothesis that phytoplankton growth and grazing losses determine, to first order, the local dynamics of phytoplankton in the upwelling circulation. Eight experiments of 3–5 days each were conducted over the course of two cruises in May–June 2006 and April 2007 following the trajectories of satellite-tracked drifters. Rates of phytoplankton growth and microzooplankton grazing were determined by daily in situ dilution incubations at 8 depths spanning the euphotic zone. Mesozooplankton grazing was assessed by gut fluorescence analysis of animals collected from net tows through the euphotic zone. We compared directly the net rates of change observed for the ambient phytoplankton community to the net growth rates predicted from experimental determinations of each process rate. The resulting relationship accounted for 91% of the variability observed, providing strong support for the growth-grazing hypothesis. In addition, grazing by mesozooplankton was unexpectedly high and variable, driving a substantial positive to negative shift in phytoplankton net rate of change between years despite comparable environmental conditions and similar high growth rates and suggesting strong top-down control potential. The demonstrated agreement between net ambient and experimental community changes is an important point of validation for using field data to parameterize models. Data sets of this type may provide an important source of new information and rate constraints for developing better coupled biological–physical models of upwelling system dynamics.

1. Introduction

Coastal upwelling ecosystems present a formidable challenge for studying the dynamics of plankton communities because they combine high spatial variability in hydrography, community composition and forcing conditions in a complex advective field. Observations at fixed locations can be hopelessly confounded by variable sources and flows of water and associated biota past the site, and by the decoupled temporal scales of relevant processes, such as nutrient uptake, primary production, grazing and export. Investigations conducted in the moving frames of reference of drogued drifters circumvent many of the inherent problems of fixed-site studies; hence, this strategy has been used productively in physical, chemical and biological studies of upwelling systems for some time (e.g., Wilkerson and Dugdale, 1987; Ishizaka and Hofmann, 1988; Abbott et al., 1990; Alvarez-Salgado et al., 2001). Nonetheless, quasi-Lagrangian experiments require substantial commitments of resources to understand the evolving characteristics of individual parcels of water and are typically done very sparingly, or, if in large numbers, with automated sampling devices (e.g., Abbott and Letelier, 1998) that cannot measure many key rate processes. In contrast, recent advances in high-resolution modeling (e.g., Gruber et al., 2006; Wainwright et al., 2007) have shown promise of providing a more synoptic understanding of ecosystem responses to spatially and temporally variable physical forcing, but such models are typically poorly constrained by the sparse data available to parameterize rate relationships and validate results. Focused efforts are therefore needed to study the natural dynamics and variability of upwelling systems not only as ends in themselves, but in ways that facilitate the development of better informed models. For process studies, this means making some effort to determine whether the field rate measurements that will ultimately go into models are consistent with observed responses of the systems being investigated.

We report here the results of field investigations of phytoplankton growth and grazing losses conducted in the coastal upwelling system off Point Conception, California as part of the California Current Ecosystem, Long-Term Ecological Research (CCE-LTER) Program. CCE-LTER has the ultimate goal of understanding climate-driven transitions in ecological state and biogeochemistry of the California Current, an objective that necessitates long-term

* Corresponding author. Tel.: +1 858 534 4702; fax: +1 858 534 6500.
E-mail address: mlandry@ucsd.edu (M.R. Landry).

0079-6611/$ - see front matter © 2009 Elsevier Ltd. All rights reserved.
doi:10.1016/j.pocean.2009.07.026

observational studies that document system trends, short-term experimental studies that elucidate processes, and ecological modeling that bridges these different time scales. The present process study addresses the hypothesis that phytoplankton growth and grazing losses determine, to first order, the local dynamics of phytoplankton standing stock in the circulation field of this upwelling system. Eight depth-profile experiments of 3–5 days each were conducted over the course of two cruises in May–June 2006 and April 2007 following the trajectories of drogued drifters, which also provided attachment sites for in situ experimental incubations spanning the euphotic zone. We compare directly the observed net changes in the ambient phytoplankton community to the net growth rates predicted from experimental determinations of each process rate. The strong 1:1 relationship observed between these independent assessments of net water-column change supports the growth-grazing hypothesis. In addition, the unexpected magnitude and variability of mesozooplankton grazing in this system is shown to drive a substantial directional shift in net phytoplankton growth between experiments conducted in these two years despite comparable environmental conditions and similar high growth rates. This study thus suggests important top-down grazing influences on phytoplankton dynamics that may need to be incorporated into models of this system to represent it accurately.

2. Methods

2.1. Study site

Experimental studies were conducted off Point Conception during two springtime cruises, the season of highest upwelling activity and system spatial variability in the Southern California region. Research operations on CCE Process cruise P0605 were conducted on R/V *Knorr* from 10 May to 5 June 2006. *Thomas G. Thompson* was the research vessel for cruise P0704 from 3 to 20 April 2007. The area of investigation extended from 10 to 400 km offshore (Fig. 1), roughly along line 80 of the California Cooperative Oceanic Fisheries Investigations (CalCOFI) program, which has a long record of time-series sampling in this region dating back to 1949.

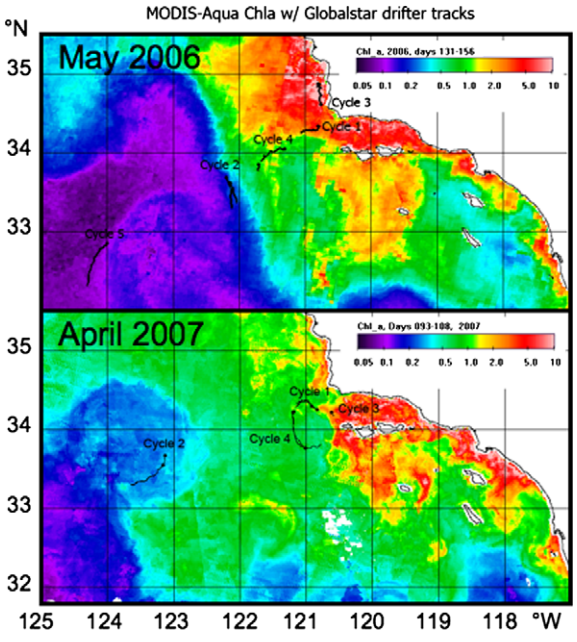

Fig. 1. Overlays of experimental cycle drifter tracks on cruise-averaged MODIS-Aqua maps of surface chlorophyll *a* for CCE Process cruises P0605 (May 2006) and P0704 (April 2007) off of Pt. Conception, California. Black dots indicate the locations of initial drifter deployments. Figure courtesy of *M.* Kahru.

Specific water parcels were selected to exploit the range of conditions that existed spatially on each cruise. Parcels were initially identified using sea surface temperature and near-surface Chl *a* imagery from MODIS-Aqua and/or SeaWifs satellites, together with subsurface ocean conditions from *Spray* ocean gliders (cf. Davis et al., 2008). The water parcels were then mapped with a Moving Vessel Profiling system (Brooke Ocean Technology, Ltd., Ohman unpubl.) and flow-through surface sampling with transects parallel and perpendicular to the directions of mean current flow to ensure that water properties were reasonably homogeneous and without major frontal features in the vicinity.

2.2. Lagrangian drift array

Experiments were conducted as activity "cycles" of 3–5 day duration (Table 1) following the path of a satellite-tracked drift array that served both to mark the mean flow of near-surface waters and as a platform for in situ bottle incubations (below). The drifter float was a WOCE SVP (World Ocean Circulation Experiment, Surface Velocity Program) design, with a top strobe light and Globalstar telemetry that recorded positions every 10 min and transmitted them at 30-min intervals (Pacific Gyre, San Diego). An Iridium backup communications system was installed, though not used, on drifters deployed on the second cruise after one drifter failed to report and was lost on the first cruise. Drift floats were attached by removable screw-on tether lines of coated 4.8-mm wire to a 3 × 1-m holey sock drogue centered at 15 m. Below the drogue, a second tether line of 3.1-mm wire extended the array to a small weight at 30, 60 or 140 m, depending on euphotic zone depth of the water parcel investigated during each activity cycle.

For bottle incubations, the drifter tethers were constructed with pairs of built-in stainless steel loops set 1 m apart and centered at standard depths: 2, 5, 8, and 12 m for the upper tether; 19, 25, 30, 35, 40, 50, and 60 m for lower tethers used in the more productive coastal stations; and at 10-m intervals from 20 to 140 m for deployments in offshore oligotrophic waters. Drag ratio calculations for the full arrays exceeded 40 (Niiler et al., 1995) for all permutations of experimental attachments at 8 depths (range = 114–125). The center of drag varied from 14.6 to 16.8 m for shallow (30–60 m) deployments, but extended from 23.6 to 24.9 m for offshore deployments with the longer bottom tether.

2.3. Phytoplankton growth and microzooplankton grazing

Rates of phytoplankton community growth and microzooplankton grazing on phytoplankton were assessed from chlorophyll *a* analyses of in situ dilution incubations following the two-treatment approach of Landry et al. (1984), as refined in Landry et al. (2008). We conducted daily profiles of unreplicated incubations at 8 depths to get daily rate estimates of depth-integrated growth and grazing, and we averaged 3–5 days of such profiles to get means and standard deviations for each experimental cycle.

For each of the daily drift array deployments, experimental incubations spanned the range of the euphotic zone, from 2–5 m at the top to a depth averaging ~0.4% of surface illumination, as determined in daytime light profiles from a CTD-mounted PAR sensor. We collected water from 8 depths (6 depths for Cycle 3, P0605) and prepared a pair of polycarbonate bottles (2.7 L) with whole seawater (100%) and 33% whole seawater (diluted with 0.1-μm filtered seawater) at each depth. Seawater was filtered directly from the Niskin bottles using a peristaltic pump, silicone tubing and an in-line Suporcap filter capsule that had previously been acid washed (10% trace-metal grade HCl followed by Milli-Q and seawater rinses). Dilution treatment bottles received pre-measured volumes of filtered water from the collection depths, and then were gently filled (silicone tubing below the water level) with

Table 1
Comparison of system characteristics for drift array experimental cycles. Distance = initial position of drifter from shore. *Z* = depth of deepest incubations sample. *T*, Sal, Nitr and Chl *a* are initial surface (2 m) values of temperature, salinity, nitrate and chlorophyll *a* for the drifter cycle. MLD = initial mixed layer depth.% I_o at *Z* = irradiance at the depth of the deepest incubation bottle (% surface irradiance). Nitracline is defined as the shallowest depth at which nitrate concentration exceeds 1 μM. Mean μ_{ML} = average (±std. dev.) growth rate of phytoplankton in the upper 1/3rd of the euphotic zone, *n* = number of experimental rate estimates for μ_{ML}.

Cycle #	Array dates	Distance (km)	Z (m)	T (°C)	Sal (psu)	Nitr (μM)	Chl a (μg L^{-1})	MLD (m)	I_o at Z (%)	Nitracline (m)	Mean μ_{ML} (d^{-1})	*n*
P0605												
1	11–15 May	29	50	11.3	33.62	13.44	2.94	25	0.07	Surface	0.51 ± 0.14	16
2	17–21 May	166	100	14.4	32.92	0.07	0.10	37	0.28	75	0.39 ± 0.17	11
3	22–25 May	11	25	13.3	33.35	1.75	6.47	15	0.66	Surface	0.33 ± 0.23	12
4	26–31 May	89	50	14.9	33.27	0.85	0.74	32	0.69	30	0.50 ± 0.13	16
5	1–5 June	356	90	16.1	33.09	0.08	0.11	35	0.26	63	0.28 ± 0.13	16
P0704												
1	4–8 April	39	50	12.4	33.70	8.59	2.25	19	0.50	Surface	0.65 ± 0.33	16
2	10–13 April	255	90	14.3	33.18	0.08	0.18	48	0.17	73	0.34 ± 0.24	14
4	15–20 April	63	50	11.8	33.70	11.07	1.10	51	0.26	Surface	0.50 ± 0.16	16

unscreened water from the Niskin bottles. The bottles were then tightly capped, placed into net bags and clipped onto attached rings at the depth of collection on the array tether line during deployment. For back-to-back deployments within an experimental cycle, we collected water adjacent to the array and set up the second set of experiments before recovering the first. Hand recovery of the array, switching of net bags and redeployment was generally completed in 15–20 min. All experiments were started with water collected at the same time of day (0200 CTD), with recovery and redeployments typically completed by ~0430 (pre-sunrise).

Rate estimates are based on initial and final subsamples (250 ml) taken for fluorometric analyses of Chl *a*. The samples were immediately filtered onto GF/F filters, and the Chl *a* extracted with 90% acetone in a dark refrigerator for 24 h. Extracted samples were shaken, centrifuged and quantified on a calibrated Turner Designs model 10 fluorometer (Strickland and Parsons, 1972).

Instantaneous rates of phytoplankton growth (μ) and microzooplankton grazing (m) were estimated as $m = (k_d - k)/(1-x)$ and $\mu = k + m$, where k and k_d are, respectively, the observed net rates of change of Chl *a* in the natural and diluted treatments and "x" = the fraction of natural grazer density in the dilute treatment. These calculations assume a linear relationship between measured grazing rate and the dilution of grazer abundance by the experimental manipulation. We tested this assumption on several occasions at the richer coastal stations using very dilute concentrations of ambient mixed-layer seawater ($\leqslant$0.1 μg Chl *a* L^{-1}; 2–8% of ambient) and found rate estimates of μ (0.57 ± 0.17 d^{-1}, n = 16) indistinguishable from those in Table 1. Areal estimates of growth and grazing rates were computed by integrating the experiment depth profiles to the deepest incubation bottles, after weighting the mean rates in each depth strata to the proportion of the total water column Chl *a* that it represented.

2.4. Mesozooplankton grazing

During drifter deployment, zooplankton net tows were taken two times a day, near 1100 and 2300, using 202-μm mesh, 0.71-m diameter bongo nets to a maximum depth of 210 m. Upon net retrieval, the collected animals were immediately anesthetized with carbon dioxide in soda water to prevent egestion of gut contents and size-fractionated into five classes (0.2–0.5, 0.5–1, 1–2, 2–5, and >5 mm) using nested sieves. Each size fraction was split with a Folsom splitter and 3/8 saved for gut fluorescence analysis, 3/8 for later determination of dry mass, and 1/4 saved for other assays. All samples were frozen in liquid nitrogen for later lab processing.

Laboratory analyses generally consisted of two 1/8 replicates of the 0.2–0.5 and 0.5–1.0 mm size fractionations, two 1/4 replicates of the 1–2 mm fraction, 1/4 of the 2–5 mm fraction, and the entire 5 mm sample. The analyzed portion of each sample was examined carefully with a dissecting microscope to remove phytoplankton, debris and micronekton. The zooplankton were then placed in test tubes with 10 ml of 90% acetone and sonicated four times for 5 s with an ultrasonic tissue homogenizer. Test tubes with acetone were kept on ice prior to use and during sonication, then placed at −20 °C in the dark for 1–3 h to extract pigments. Test tubes were centrifuged for 10 min at 1600 g, and two 4-ml replicates of the supernatant were separated into cuvettes and allowed to warm in the dark to room temperature prior to fluorometric analysis. A calibrated Turner Designs model 10 fluorometer was used for the analysis of chlorophyll and derivative pigments, before and after acidification with two drops of 10% HCl. Tissue fluorescence blanks determined by starving mesozooplankton in filtered seawater for 24 h, then fractionating into the five size classes and freezing and analyzing as above, were subtracted from experimental determinations to obtain gut fluorescence.

Following Conover et al. (1986), who demonstrated that standard fluorometric equations compute phaeopigment values in terms of chlorophyll weight equivalents, we did not multiply phaeopigment estimates by 1.51 (the Chl *a*:phaeopigment weight ratio) as has sometimes been done for gut fluorescence assessments of mesozooplankton grazing (e.g., Båmstedt et al., 2000). Based on arguments by Durbin and Campbell (2007), we also assumed that pigment degradation to non-fluorescent products during the digestive process is inherently accounted for in experimental determinations of gut clearance rate. For these, we used the temperature-dependent function of Dam and Peterson (1988), K (min^{-1}) = 0.0124 $e^{0.07675\ T\ (°C)}$, where K is the instantaneous rate of gut pigment turnover and T is temperature at the depth of the chlorophyll maximum layer, where zooplankton were assumed to concentrate and feed most actively on phytoplankton. From the above, daily ingestion (DI) of Chl *a* by the mesozooplankton community was calculated as the sum of the day–night means of Chl *a* and phaeopigment from pigment analyses for all zooplankton size fractions multiplied times the temperature-dependent gut pigment turnover rate [=K (min^{-1}) * 1440 min d^{-1}]. To be consistent with microzooplankton grazing estimates, the grazing impacts of mesozooplankton (M, d^{-1}) are presented here as daily instantaneous rates of loss of Chl *a* over the depth range of the euphotic zone (= $\ln[(Chl_o - DI)/Chl_o]$, where Chl_o is the depth-integrated concentration of Chl *a*).

3. Results

3.1. Experimental conditions

The differing environmental contexts of the drifter experiments are evident in Fig. 1, which superimposes the drifter tracks onto MODIS-Aqua satellite composites of surface Chl *a* for the time

intervals of each cruise. During the May 2006 cruise (P0605), Cycle 1 appeared to capture a water parcel with a recent upwelling history, as determined by low SST and high surface NO_3 concentration (Table 1), which was advecting directly offshore (to the west). Cycle 2 was located in the core of the southward flowing California Current (as defined by reduced salinity) and provided sharply contrasting conditions to Cycle 1, with low surface Chl *a* and a deep nitracline (Table 1). The two drift paths that are evident for Cycle 2 represent a restarting of the experiment after the initial drifter moved into restricted waters. Rate estimates for the two parts of this cycle were separately computed, then averaged, for the present analysis. Cycle 3 was run in northward flowing (inshore countercurrent) coastal waters, an area of high Chl *a* dominated by large dinoflagellates. This location was out of the main area of interest, and in retrospect was suboptimal for this type of experiment. Water depth increased substantially during the deployment, and there are indications that the drifter slipped relative to biological gradients. The Cycle 4 experiment was initiated downstream of the drifter trajectory from Cycle 1. While the same water is unlikely to be sampled, the lower nitrate and Chl *a* and deepening nitracline at the start of this experiment (Table 1) may represent a more evolved state of waters flowing offshore from the Pt. Conception upwelling center. Cycle 5 was meant to capture offshore oligotrophic conditions for this late spring cruise. Upper euphotic zone characteristics were similar to those in Cycle 2 (Table 1), but this location had an anomalously developed deep Chl *a* maximum (up to 1.1 μg Chl *a* L^{-1}, which was also a strong subsurface maximum in phytoplankton biomass) at 70 m relative to what is typically observed in this region.

For the April 2007 cruise (P0704), the Cycle 1 experiment began close to the location of Cycle 1 for P0605, and surface waters were similarly rich in nitrate and Chl *a* (Table 1). Net drifter displacements were also similar (offshore) for these two experiments (Fig. 1), though the drift array on P0704 initially took a northward path before turning west. Cycle 2, the only offshore experiment on the shorter 2007 cruise, was located in a warm-core anticyclonic eddy with a deep nitracline. Cycle 3 was conducted south of Point Conception during a period of strong northerly winds and was therefore expected to follow the offshore transport of a parcel originating closer to the upwelling source than previously sampled. However, this drifter immediately veered south and east, and had to be quickly rescued from shoals of the northern Channel Islands. As for the 2006 cruise, Cycle 4 began downstream of the drift path of Cycle 1. In this case, however, storm conditions between the two cycles had sharply deepened the mixed layer, cooling the surface waters and infusing them with more nitrate (Table 1). Nonetheless, the drifter trajectories of these two experiments suggest that they may be linked by entrainment in a cyclonic eddy that often occurs off of Pt. Conception (Fig. 1; Davis et al., 2008).

On closer inspection of Fig. 1, two drifter trajectories can be barely discerned for experiments conducted in April 2007. The second path was for a sediment trap array (drogue at 15 m, multitraps at 100 m) that was deployed for the full experimental cycle, rather than being recovered and redeployed daily. While results from trap deployments will not be considered here, the close correspondence between the two drifter tracks indicates that the flow fields were reasonably coherent over the scale of several kilometers and 3–5 days.

3.2. Phytoplankton growth

Over the range of environmental conditions investigated, specific growth rates of phytoplankton in the upper euphotic zone varied by about a factor of 2, from 0.3 to 0.6 d^{-1} (Table 1). We take these estimates to be indicative of maximal light-saturated rates for these waters, given other growth limiting constraints. In the classic sense that higher temperature should enhance physiological rates, temperature effects per se do not explain the growth rate differences. Faster growth is observed where surface nitrate concentration is high, which typically coincides with lower SST. Although growth rate differences between eutrophic coastal and oligotrophic offshore waters are not dramatic, standing stocks differed up to 30-fold, making the absolute rates of phytoplankton Chl *a* synthesis, and presumably biomass production, in the offshore waters a small fraction (average = 4%) of those in coastal surface waters.

Depth distributions of specific growth rate share some similarities among experiments. Maximum growth rates tend to occur in the upper 15–20 m of coastal waters with significant surface nutrients, and this stretches to 30–40 m in offshore waters in proportion to the deepening euphotic zone (Fig. 2). With one exception (Cycle 2, P0704), near-surface estimates of growth rate are also similarly depressed in these incubations, which may be a consequence of exposing mixed-layer phytoplankton to high irradiance for the full photocycle (i.e., photoadaptation of cellular pigment concentration). The growth rate profile for P0605 Cycle 4 stands out with respect to those for the other coastal experiments (top panels in Fig. 2) in having its highest growth rates substantially deeper in the water column, between 20 and 30 m. Among the experiments in this comparison, P0605 Cycle 4 is the only one with a notable subsurface nitracline, which occurred at about 30 m. The small subsurface growth rate maximum observed at a depth of 60 m during P0605 Cycle 5 is noteworthy as well. This secondary subsurface maximum was observed for all in situ incubations during Cycle 5. It coincided with the upper shoulder of the strong Chl *a* maximum and with the sharp nitracline at about 60 m (Table 1).

Depth-integrated rates of phytoplankton growth reflect the depth distributions of Chl *a* as well as those of specific growth rates. That is, the presence of substantial Chl *a* deep in the water column, where specific growth rates are low, depresses depth-integrated estimates of growth at offshore oligotrophic stations relative to coastal conditions where the highest growth and highest Chl *a* co-occur in the upper mixed layer. Since the integration does more than stretch differences in maximal growth rates (i.e., Table 1) to deeper euphotic depths, there is a clear decrease of about a factor of three in depth-integrated growth rate from coastal to offshore stations (Fig. 3).

3.3. Grazing rates

For the present analysis, we consider only the depth-integrated rates of microzooplankton grazing on Chl *a*, which are directly comparable to the water-column integrated rates for mesozooplankton grazing. Computed daily ratios of meso to microzooplankton grazing impact (Fig. 4) show the expected dominance of microherbivory (i.e., ratios <1.0) in offshore oligotrophic waters. Microzooplankton grazing on phytoplankton exceeds the impact of mesozooplankton by factors of 2–5 or more in such waters. The relative grazing contribution of mesozooplankton increased from offshore to inshore for both cruise years, but the difference was particularly striking for P0704 Cycles 1 and 4, where grazing estimates for net-collected herbivores dominated grazing (Fig. 4).

3.4. Predicted and observed net growth rates

When comparing mean depth-integrated rates of growth and grazing for all experiments (Fig. 5), it is evident that results for the two cruises differ mainly in the dramatically increased grazing impact of mesozooplankton in the coastal experiments in 2007. On average, instantaneous rates of microzooplankton grazing are a little higher for experiments conducted in the richer coastal waters, but the onshore–offshore variability is not substantial, and the

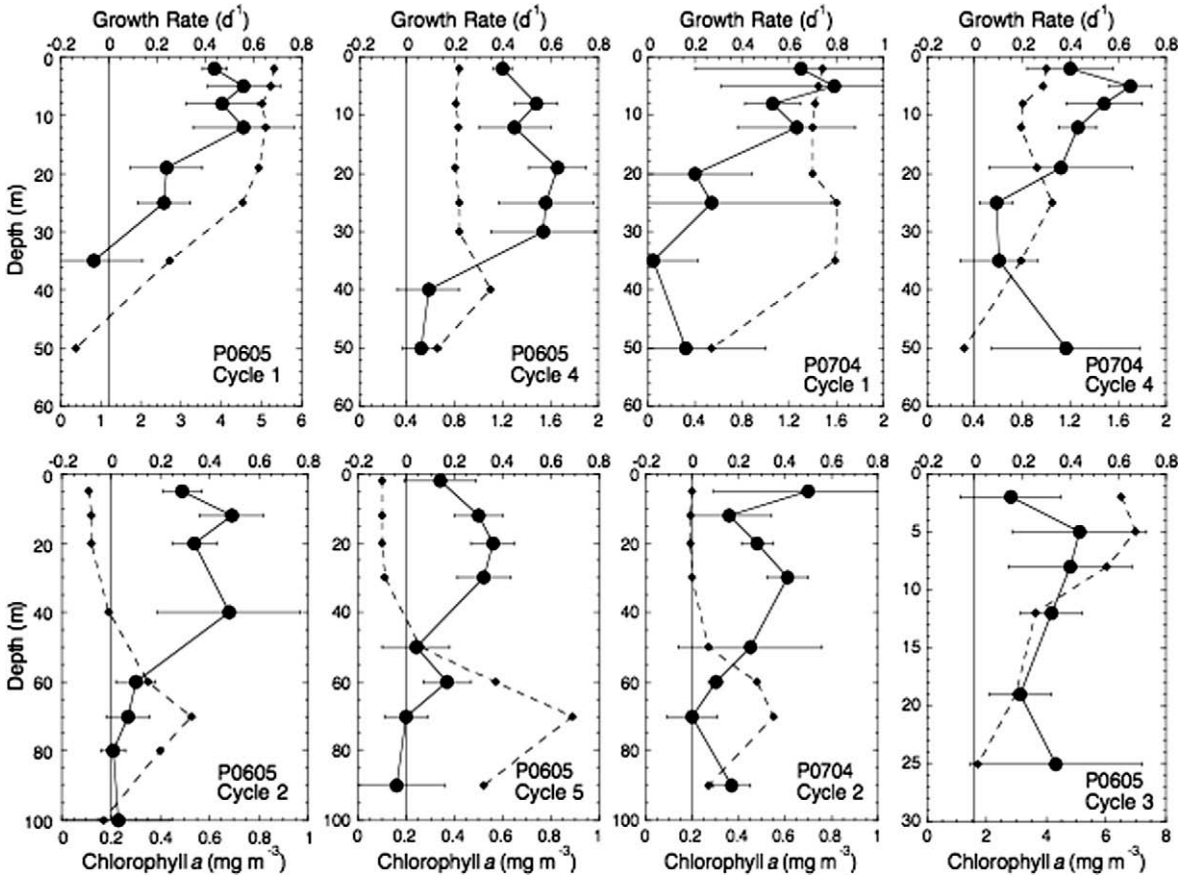

Fig. 2. Mean depth profiles of phytoplankton growth rates during CCE Process cruises P0605 and P0704. Error bars are standard deviations of rate estimates for daily experiments incubated in situ below the drogued drifter. Dashed lines and bottom axes labels show mean depth profiles of Chl *a* during the experimental cycles.

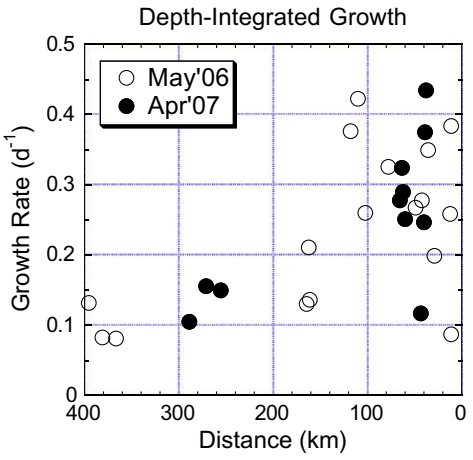

Fig. 3. Daily depth-integrated rates of phytoplankton community growth rate relative to distance offshore for drifter experiments in May 2006 and April 2007.

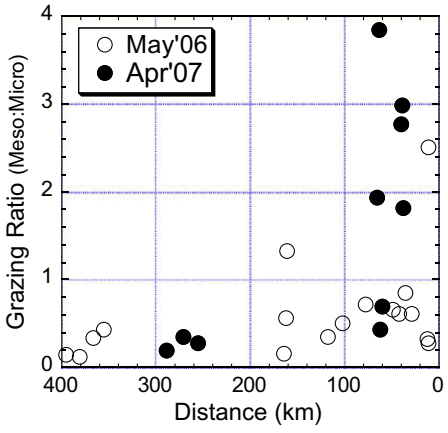

Fig. 4. Ratios of daily depth-integrated grazing rates of mesozooplankton and microzooplankton relative to distance offshore for drifter experiments in May 2006 and April 2007.

highest integrated rates (~0.2 d^{-1}) are similar between years. In the offshore region, microzooplankton grazing by itself was comparable to or exceeded phytoplankton growth rate. In richer coastal waters, it accounted for half or less of phytoplankton growth. In contrast, the mean specific rate of phytoplankton mortality due to mesozooplankton grazing during P0704 Cycle 1 was about a factor of 5 greater than during P0605 Cycle 1. These experiments were conducted at comparable distances from shore and with similar initial conditions of surface nutrients and Chl *a*. Given the similar mean rates of phytoplankton growth and microzooplankton grazing for these two experiments, variation in the magnitude of mesozooplankton grazing is principally responsible for the sign switch in calculated net phytoplankton growth observed in coastal waters, from positive (accumulating phytoplankton) in 2006 to negative (declining phytoplankton) in 2007. The predictions of these experimentally determined rate estimates are borne out by observed net changes in Chl *a* standing stock from daily water-column sampling in the drifter path (Fig. 5). Overall, our experimental rate estimates

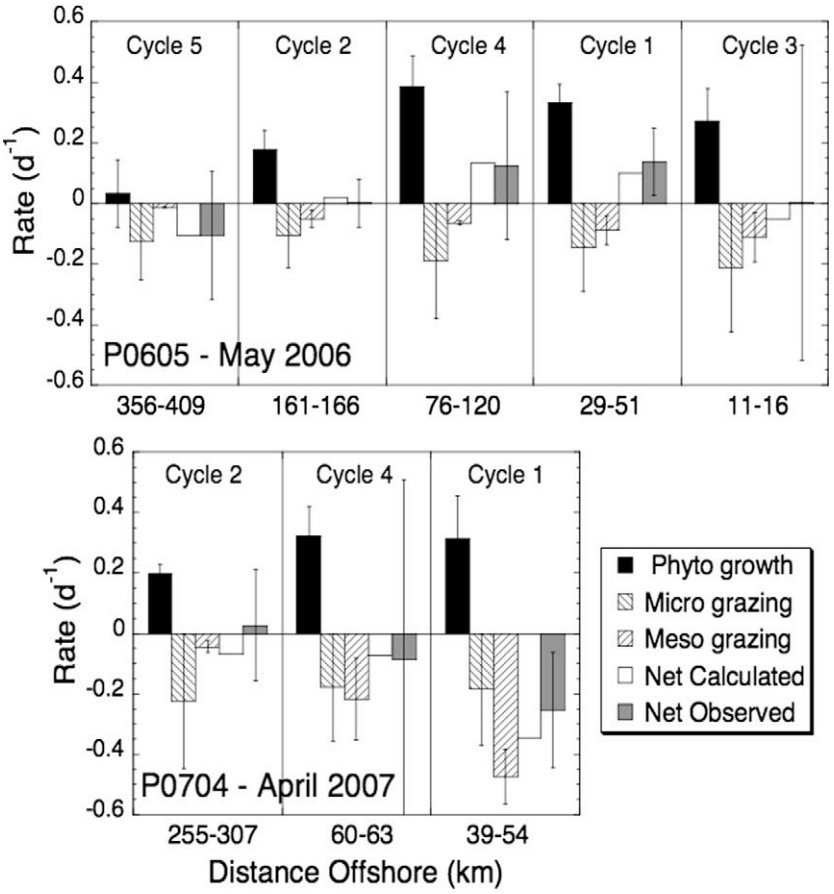

Fig. 5. Instantaneous rates of change of Chl *a* due to phytoplankton growth and micro and mesozooplankton grazing for Lagrangian drifter experiments during CCE Process cruises P0605 and P0704. Cycles are arranged West (left) to East (right) for each cruise. *X*-axis gives the range of drifter distance offshore for each experimental cycle. Phytoplankton specific growth rates (μ) and microzooplankton specific grazing rates (m) are calculated from experimental determinations of growth and grazing rates inside incubation bottles suspended in situ. Mesozooplankton specific grazing (M) is calculated from gut fluorescence. The net calculated change (k') is the resultant of μ–m–M. The net observed change is from daily measurements in the ambient water column. All rates are depth integrated and normalized to the depth distribution of Chl *a*.

for growth and grazing processes do a relatively good job of predicting observed trends in the ambient water column, explaining 90.6% of the variability observed over time scales of 3–5 days (Fig. 6). They therefore provide strong support for the notion that rates of change of phytoplankton concentration, within the context of the physical flow regime, are principally determined by the local balance of growth rates and grazing loss processes.

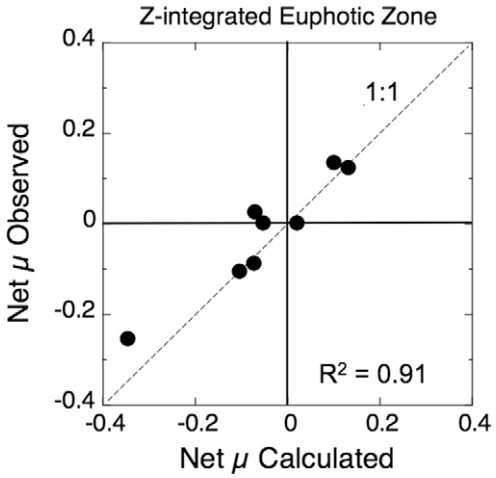

Fig. 6. Comparison of observed in situ changes of phytoplankton Chl *a* to net changes computed from experimental determinations of growth and grazing rates. All rate estimates are based on depth-integrated estimates of Chl *a* for the euphotic zone averaged over 3–5 days of drifter deployment.

4. Discussion

4.1. Experimental interpretations

The good agreement found between experimental determinations of phytoplankton growth and grazing processes and net changes of the ambient phytoplankton community in the Pt. Conception upwelling area is a major result of this study with implications for the understanding of system dynamics as well as methods. It suggests, for example, that losses due to direct sinking of phytoplankton from the euphotic zone, a process not considered in this analysis, is of relatively modest consequence in this system relative to grazing losses. This could be because new production in the core of the upwelling, where we see the highest variability in net community change, is strongly decoupled from export processes, as Olivieri and Chavez (2000) have concluded from a modeling study of plankton dynamics in the upwelling system off Monterey Bay, California. In the Olivieri and Chavez (2000) study, which sought to simulate long-term mean patterns in production, nitrate and phytoplankton concentration rather than short-term dynamics, lateral advection of production was indicated to be a dominant process over vertical export flux, and even more than local grazing. Plattner et al. (2005) have also suggested that new production in the nearshore California Current may be exported

considerable distances horizontally prior to contributing to export flux. In our experiments, drifters were used specifically to move in the frame of reference of lateral advective flux so that we could focus effectively on other processes of interest.

Low losses of phytoplankton production to direct sinking may also be indicative of a phytoplankton community composition that is not particularly conducive to sinking. In this regard, extensive microscopical analyses of the communities sampled in our experiments reveals that they were dominated by picophytoplankton and small flagellates in the offshore and small and large flagellates (dinoflagellates in the larger size fractions) in the richer coastal waters (A. Taylor and M. Landry, unpubl.). Diatoms, the phytoplankton functional group most closely associated with aggregate formation and mass sinking (Sarthou et al., 2005), accounted for 22% or less of total autotrophic C biomass in individual experiments and averaged 12% of the total for the five coastal experiments reported here. In addition, the specific conditions encountered in our coastal experiments, with generally high nitrate concentrations and silicic acid concentrations up to 15 μM (not less than 3 μM) in surface waters, would not be expected to produce unhealthy diatom cells that initiate aggregate formation. Aggregation of picoplankton cells into larger and more rapidly sinking or more edible particles may not have been significant in this system because of high cell densities and hence time necessary for aggregation reactions to develop (Richardson and Jackson, 2007).

Lastly, our experimental water parcels were generally chosen carefully to avoid fronts and major water mass transitions that could confound interpretations. Convergent frontal features would be logical places to investigate subduction processes that potentially move significant phytoplankton biomass from surface to deep waters without going first through zooplankton grazers in the euphotic zone.

Despite the careful choice of study conditions, we are mindful that the movement of water around and under a drogued drifter is not uniform at all depths, and in fact can vary greatly. Our experiments thus do not relate easily to the dynamics of a contiguous euphotic zone, but rather to the general state of a more broadly defined system as influenced by complex flows. Resampling the water column daily for process experiments, with a new set of bottle incubations and zooplankton net collections, helps to smooth the transition from the water column that was sampled initially to what was ultimately present under the drifter after 3–5 days. We are probably also fortunate that net depth-integrated rates for experiments in the more dynamic coastal area were determined largely by the combination of high phytoplankton concentration and high process rates in the upper euphotic zone, where the array was drogued. Intuitively, one would expect much greater difficulty linking ambient net community changes to measured process rates in water columns where the feature of interest (e.g., development of a deep chlorophyll maximum) is significantly separated from the drogued depth stratum. We note that a completely independent check on our phytoplankton specific growth rates comes from ocean glider-based measurements following the same parcel of water as tracked by the drifter (Davis et al., 2008). In that study, the net rate of change of Chl *a* observed in situ in the upper 25 m was 0.20 d^{-1}, which compares favorably with a mean measured here of 0.18 d^{-1} for the same depth stratum.

4.2. Growth regulation

The phytoplankton growth rates estimates from this study, which ranged on average from about one-half to one doubling of biomass per day in the upper euphotic zone, seem reasonable relative to what we might expect for mixed communities, natural photocycles and surface water temperatures of 11–16 °C (Eppley, 1972). Still, these could be low estimates to the extent that they do not account for processes, such as viral-induced mortality or programmed cell death (e.g., Bidle and Falkowski, 2004; Baudoux et al., 2007; Franklin et al., 2006). Because such processes affect equally the populations in diluted and non-diluted treatments, they would generally be invisible to the dilution incubation technique that was used here for growth rate assessments. A full accounting of processes affecting the dynamics of phytoplankton in this coastal upwelling system might therefore well include other terms for non-grazing losses.

The present study also does not clearly resolve the factors that regulate the growth rates measured. That is, while the patterns of rate depth profiles (Fig. 2) and experimental differences in mean growth rates (Table 1) are clearly suggestive of significant light and nitrate influences, the details of growth regulation may be complicated by trace-element effects. For instance, based on shipboard iron (Fe) addition experiments in the area of our drifter experiments (50–200 km offshore of Pt. Conception), King and Barbeau (2007) have demonstrated responses of nutrient drawdown, Chl *a* and phytoplankton community composition that are consistent with Fe limitation. Following a similar approach during CCE Process cruise P0605, A. King (unpubl.) found that Fe limitation was initially not evident at the start of Cycle 1 but developed at the end. Fe limitation was also found during the initial and final days of the Cycle 4 experiment. From such results, we can reasonably surmise that the presence of excess nitrate in surface waters during our experiments does not ensure that the phytoplankton were entirely nutrient replete. Indeed, the interesting subsurface maximum in growth rate observed during P0605 Cycle 4 may have less to do with nitrate per se and more about a source of new Fe in the nitracline at 30 m.

The strongly developed deep Chl *a* maximum (DCM) encountered during P0605 Cycle 5 is also among the sites where Fe and light were recently shown to co-limit phytoplankton growth rate by Hopkinson and Barbeau (2008; results of experiments at this site are shown in their Figs. 8 and 9 and associated tables as Station KN1). Assuming that the upper euphotic zone could have unused Fe from aeolian deposition at this location because major nutrients are severely depleted there, our experimental incubations on the upper shoulder of the DCM (60 m) may well have captured the optimal location in the water column where light and Fe from above have mixed with sufficient nitrate (from below) to support the secondary peak in growth rate observed (Fig. 2). This speculation differs from the mechanistic interpretation of Hopkinson and Barbeau (2008) in that it requires a third co-limiting component (nitrate) for optimal effect. Hopkinson and Barbeau (2008) tested their light-Fe co-limitation hypothesis at this station with deeper water from the DCM (78 m) where nitrate concentration (4.1 μM) was clearly not limiting.

4.3. Grazing relationships

Microzooplankton generally dominated grazing processes for the experiments conducted, though results differed in some respects from expectations derived from the dilution synthesis of Calbet and Landry (2004). Specifically, we found a portion of our study site, roughly where our Cycles 1 and 4 experiments were conducted (30–100 km offshore), where the grazing impact of microzooplankton averaged 40% of phytoplankton growth, rather than the 60% suggested by Calbet and Landry (2004) for coastal stations. Interestingly, the grazing rate ratio for the innermost drift experiment (P0605 Cycle 3) was 78%, which suggests that the critical determinant of this ratio is not simply distance to shore or system richness. Before considering what these differences may mean ecologically, it is worth noting that our ability

simply to see them is a matter of numbers. The Calbet and Landry (2004) synthesis was based on the analysis of 788 experiments conducted throughout the global oceans, of which 142 were classified as *coastal*. For the present analysis, we have compiled the results of 235 independent incubations for just one coastal ecosystem. If we average all of these data, the mean grazing ratio for the California Current Ecosystem is 70%, not different from the global ocean average of 67%. It is only due to the larger numbers involved and multiple cruises and days of experiments that we are able to see a more detailed pattern emerge.

One hypothesis that might explain the chronically low grazing impact of microzooplankton in the coastal core region of our study site is that predator cropping keeps them at concentrations lower than needed to exert a higher level of grazing. It seems unlikely that phytoplankton community size structure by itself would account for such an effect, since systems clearly exist (including portions of the Southern Ocean) in which high grazing impact of microzooplankton and abundant large diatoms are compatible (Landry et al., 2002). The present experiments did not assess the direct predatory impact of mesozooplankton on heterotrophic protists, but they do show a very high and variable mesozooplankton grazing impact on phytoplankton that speaks to the potential for top-down control. That mesozooplankton grazing impact should be so strong as to drive a negative rate of change of rapidly growing phytoplankton in high nitrate surface water is an important and unexpected result of this study, and one can only speculate as to the specific environmental conditions that led to the much higher zooplankton biomass and grazing in April 2007 compared to May 2006. Does a month make that much of a difference when growth conditions for phytoplankton (Table 1) were otherwise similar overall between years? Do top-down impacts of higher-level consumers (e.g., pelagic fish) in this area determine variability in mesozooplankton grazing? Are mesoscale circulation features that set up offshore of the Channel Islands off of Pt. Conception potentially important for concentrating zooplankton and grazing potential in this region? The results of this study have left many open questions for future investigation by field experiments and models.

5. Conclusions

Our study is the first coherent investigation of phytoplankton growth and zooplankton grazing interactions across a range of environmental conditions in a coastal upwelling ecosystem. Following the paths of quasi-Lagrangian drifters, we have shown that experimentally derived estimates of phytoplankton community growth, microzooplankton grazing and mesozooplankton grazing, all based on Chl *a* and integrated for the euphotic zone, can explain a large fraction (91%) of the variability observed in the net changes of ambient Chl a over time scales of 3–5 days. Since community-level dynamics are shown to be tightly constrained by experimental rate measurements for this system, detailed analyses of population-specific measurements that were made also for these experiments will likely be fruitful in elucidating the contributions of individual populations to community dynamics and how they vary across the range of environmental conditions sampled. The demonstrated agreement between net ambient observations and experimentally predicted changes is an important point of validation for using field data to parameterize models. Data sets of this type may therefore provide an important source of new information and rate constraints for developing better coupled biological–physical models of upwelling system dynamics.

Acknowledgements

We greatly appreciate the professionalism and can-do attitudes of the captain and crews of the R/Vs *Knorr* and *T.G. Thompson*, who made this work possible under sometimes challenging sea conditions. We also thank R. Rykaczewski, M. Decima, J. Powell, D. Taniguchi and others involved in the shipboard zooplankton sampling and initial sample processing, and M. Roadman, N. Spear, D. Balch and K. Lee, who assisted with experimental set up, filtrations and chlorophyll analyses. We are especially grateful to M. Kahru for producing Fig. 1 as well as his support of cruise activities with satellite mapping. This work was supported by National Science Foundation funding (OCE 04-17616) for the California Current Ecosystem LTER site.

References

Abbott, M.R., Letelier, R.M., 1998. Decorrelation scales of chlorophyll as observed from bio-optical drifters in the California Current. Deep-Sea Research, Part 2 45, 1639–1667.

Abbott, M.R., Brink, K.H., Booth, C.R., Blasco, D., Codispoti, L.A., Niiler, P.P., Ramp, S.R., 1990. Observations of phytoplankton and nutrients from a Lagrangian drifter off northern California. Journal of Geophysical Research, Oceans 95, 9393–9409.

Alvarez-Salgado, X.A., Doval, M.D., Borges, A.V., Joint, I., Frankignoulle, M., Woodward, E.M.S., Figueiras, F.G., 2001. Off-shelf fluxes of labile materials by an upwelling filament in the NW Iberian Upwelling System. Progress in Oceanography 51, 321–337.

Båmstedt, U., Gifford, D.J., Irigoien, X., Atkinson, A., Roman, M., 2000. Feeding. In: Harris, R.P., Wiebe, P.H., Lenz, J., Skjodal, H.R., Huntley, M. (Eds.), ICES Zooplankton Methodology Manual. Academic Press, London, pp. 297–399.

Baudoux, A.-C., Veldhuis, M.J.W., Witte, H.J., Brussaard, C.P.D., 2007. Viruses as mortality agents of picophytoplankton in the deep chlorophyll maximum layer during IRONAGES III. Limnology and Oceanography 52, 2519–2529.

Bidle, K.D., Falkowski, P., 2004. Cell death in planktonic, photosynthetic microorganisms. Nature Reviews: Microbiology 2, 643–655.

Calbet, A., Landry, M.R., 2004. Phytoplankton growth, microzooplankton grazing and carbon cycling in marine systems. Limnology and Oceanography 49, 51–57.

Conover, R.J., Durvasula, R., Roy, S., Wang, R., 1986. Probable loss of chlorophyll-derived pigments during passage through the gut of zooplankton, and some of the consequences. Limnology and Oceanography 31, 878–887.

Dam, H.G., Peterson, W.T., 1988. The effect of temperature on the gut clearance rate constant of planktonic copepods. Journal of Experimental Marine Biology and Ecology 123, 1–14.

Davis, R.E., Ohman, M.D., Rudnick, D.L., Sherman, J.T., Hodges, B., 2008. Glider surveillance of physics and biology in the southern California Current System. Limnology and Oceanography 53, 2151–2168.

Durbin, E.G., Campbell, R.G., 2007. Reassessment of the gut pigment method for estimating in situ zooplankton ingestion. Marine Ecology Progress Series 331, 305–307.

Eppley, R.W., 1972. Temperature and phytoplankton growth in the sea. Fishery Bulletin 70, 1063–1085.

Franklin, D.J., Brussaard, C.P.D., Berges, J.A., 2006. What is the role and nature of programmed cell death in phytoplankton ecology? European Journal of Phycology 41, 1–14.

Gruber, N., Frenzel, H., Doney, S.C., Marchesiello, P., McWilliams, J.C., Moisan, J.R., Oram, J.J., Plattner, G.-K., Stolzenbach, K.D., 2006. Eddy-resolving simulation of plankton ecosystem dynamics in the California Current System. Deep Sea Research, Part I 53, 1483–1516.

Hopkinson, B.M., Barbeau, K., 2008. Interactive influences of iron and light limitation on phytoplankton at subsurface chlorophyll maxima in the eastern North Pacific. Limnology and Oceanography 53, 1303–1318.

Ishizaka, J., Hofmann, E.E., 1988. Plankton dynamics on the outer southeastern US continental shelf. Part 1. Lagrangian particle tracing experiments. Journal of Marine Research 46, 853–882.

King, A.L., Barbeau, K., 2007. Evidence for phytoplankton iron limitation in the southern California Current System. Marine Ecology Progress Series 342, 91–103.

Landry, M.R., Haas, L.W., Fagerness, V.L., 1984. Dynamics of microplankton communities: experiments in Kaneohe Bay, Hawaii. Marine Ecology Progress Series 16, 127–133.

Landry, M.R., Selph, K.E., Brown, S.L., Abbott, M.R., Measures, C.I., Vink, S., Allen, C.B., Calbet, A., Christensen, S., Nolla, H., 2002. Seasonal dynamics of phytoplankton in the Antarctic Polar Front region at 170°W. Deep-Sea Research, Part II 49, 1843–1865.

Landry, M.R., Brown, S.L., Rii, Y.M., Selph, K.E., Bidigare, R., Yang, E.J., Simmons, M.P., 2008. Depth-stratified phytoplankton dynamics in Cyclone *Opal*, a subtropical mesoscale eddy. Deep-Sea Research, Part II 55, 1348–1359.

Niiler, P.P., Sybrandy, A.S., Bi, K., Poulain, P.M., Bitterman, D., 1995. Measurements of the water-flowing capability of holey-sock and TRISTAR drifters. Deep-Sea Research 42, 1951–1964.

Olivieri, R.A., Chavez, F.P., 2000. A model of plankton dynamics for the coastal upwelling system of Monterey Bay, California. Deep-Sea Research, Part 2 47, 1077–1106.

Plattner, G.K., Gruber, N., Frenzel, H., McWilliams, J.C., 2005. Decoupling marine export production from new production. Geophysical Research Letters 32 (Art. No. L11612).

Richardson, T.L., Jackson, G.A., 2007. Small phytoplankton and carbon export from the surface ocean. Science 315, 838–840.

Sarthou, G., Timmermans, K.R., Blain, S., Treguer, P., 2005. Growth physiology and fate of diatoms in the ocean: a review. Journal of Sea Research 53, 25–42.

Strickland, J.H., Parsons, T.R. 1972. A practical handbook of seawater analysis, second ed. Bulletin of the Fisheries Research Board of Canada, 167.

Wainwright, T.C., Feinberg, L.R., Hooff, R.C., Peterson, W.T., 2007. A comparison of two lower trophic models for the California Current System. Ecological Modelling 202, 120–131.

Wilkerson, F.P., Dugdale, R.C., 1987. The use of large shipboard barrels and drifters to study the effects of coastal upwelling on phytoplankton dynamics. Limnology and Oceanography 32, 368–382.